

# Enhanced bioavailability and efficiency of curcumin for the treatment of asthma by its formulation in solid lipid nanoparticles

Wenrui Wang<sup>1,\*</sup>Rongrong Zhu<sup>1,\*</sup>Qian Xie<sup>1</sup>Ang Li<sup>1</sup>Yu Xiao<sup>1</sup>Kun Li<sup>1</sup>Hui Liu<sup>2</sup>Daxiang Cui<sup>3</sup>Yihan Chen<sup>1</sup>Shilong Wang<sup>1</sup>

<sup>1</sup>East Hospital, School of Life Science and Technology, Tongji University, Shanghai, People's Republic of China;

<sup>2</sup>Eastern Hepatobiliary Surgery Hospital, Second Military Medical University, Shanghai, People's Republic of China; <sup>3</sup>National Key Laboratory of Nano/Micro Fabrication Technology, Shanghai Jiao Tong University, Shanghai, People's Republic of China

\*These authors contributed equally to this study

Correspondence: Shilong Wang  
School of Life Science and Technology,  
Tongji University, 1239 Siping Road,  
Shanghai 200092, People's Republic  
of China  
Tel +86 21 659 82595  
Fax +86 21 659 82286  
Email wsl@tongji.edu.cn

Hui Liu  
Eastern Hepatobiliary Surgery Hospital,  
Second Military Medical University,  
Shanghai 200438, People's Republic  
of China  
Tel +86 21 818 75463  
Fax +86 21 655 62400  
Email liuhuigg@hotmail.com

**Abstract:** Curcumin has shown considerable pharmacological activity, including anti-inflammatory, but its poor bioavailability and rapid metabolism have limited its application. The purpose of the present study was to formulate curcumin-solid lipid nanoparticles (curcumin-SLNs) to improve its therapeutic efficacy in an ovalbumin (OVA)-induced allergic rat model of asthma. A solvent injection method was used to prepare the curcumin-SLNs. Physicochemical properties of curcumin-SLNs were characterized, and release experiments were performed in vitro. The pharmacokinetics in tissue distribution was studied in mice, and the therapeutic effect of the formulation was evaluated in the model. The prepared formulation showed an average size of 190 nm with a zeta potential value of  $-20.7$  mV and 75% drug entrapment efficiency. X-ray diffraction analysis revealed the amorphous nature of the encapsulated curcumin. The release profile of curcumin-SLNs was an initial burst followed by sustained release. The curcumin concentrations in plasma suspension were significantly higher than those obtained with curcumin alone. Following administration of the curcumin-SLNs, all the tissue concentrations of curcumin increased, especially in lung and liver. In the animal model of asthma, curcumin-SLNs effectively suppressed airway hyperresponsiveness and inflammatory cell infiltration and also significantly inhibited the expression of T-helper-2-type cytokines, such as interleukin-4 and interleukin-13, in bronchoalveolar lavage fluid compared to the asthma group and curcumin-treated group. These observations implied that curcumin-SLNs could be a promising candidate for asthma therapy.

**Keywords:** airway hyperresponsiveness, pharmacokinetics, curcumin, solid lipid nanoparticles

Asthma is one of the most common chronic inflammatory diseases. According to the latest report of World Health Organization,<sup>1</sup> about 300 million people worldwide have suffered from asthma. Asthma is characterized by airway hyperresponsiveness (AHR), multicellular inflammation, and airway obstruction and is accompanied by intermittent episodes of wheezing and coughing.<sup>2,3</sup> Inhaled corticosteroids provide one of the most effective curative therapies, but this method has severe side effects with long-term use,<sup>4-6</sup> such as hypertension, cataracts, osteoporosis in elderly patients, and stunted growth in children. However, inhaled corticosteroids are still required in the systemic administration of glucocorticoids for intractable asthma or asthmatic exacerbation.<sup>7</sup> When glucocorticoids are administered intravenously, they are first metabolized in the lungs, which leads to a greater amount and more frequent administration to reach a valid treatment concentration at the sites of disease.<sup>8</sup> Therefore, one important concept for reducing systemic side effects is to find candidate drugs with prolonged

pulmonary efficacy and minimal systemic exposure. In this regard, there is an urgent need to explore novel agents for asthma therapy.

Curcumin is a yellow polyphenol compound isolated from the rhizomes of *Curcuma longa*, a plant that grows in India, China, and Southeast Asia.<sup>9,10</sup> In the past few years, studies have shown that curcumin has potential therapeutic value in a variety of chronic diseases, including asthma.<sup>11</sup> Previous studies have shown that curcumin inhibited ovalbumin (OVA)-induced airway constriction and airway hyperreactivity and airway inflammation in a murine model of asthma through suppression of nitrous oxide.<sup>12,13</sup> Recent studies further indicated that curcumin might attenuate the development of asthma by inhibition of nuclear factor- $\kappa$ B activation.<sup>14</sup> Although curcumin has been demonstrated to have anti-inflammatory potential in various therapies, its extremely low aqueous solubility, rapid metabolism, low gastrointestinal absorption, and degradation at alkaline pH limit its bioavailability and clinical efficacy.<sup>15–17</sup> As a result, a drug carrier system that can deliver curcumin to the inflamed regions for sustained release would be a potential approach for asthma treatment.

Solid lipid nanoparticles (SLNs) have attracted increasing attention as a potential drug-delivery carrier because of their unique structure and properties, such as good biocompatibility, protection for the incorporated compound against degradation, and controlled release of drugs.<sup>18,19</sup> Curcumin loaded in transferrin-mediated SLNs could enhance its anticancer effect on breast cancer cells in vitro.<sup>20</sup> Previous studies have demonstrated the potential of curcumin-SLNs for treatment of Alzheimer's disease in male *Lacca* mice.<sup>21</sup>

In this study, our aim was to investigate the therapeutic effect of curcumin-SLNs in the treatment of asthma. Curcumin loaded in SLNs was prepared using the solvent injection method. The physiochemical characteristics in an in vitro release study were also evaluated. The pharmacokinetics and biodistribution of curcumin-SLNs in mice were investigated by high performance liquid chromatography. Finally, the therapeutic efficacy of the curcumin-SLNs was tested in a murine asthma model.

## Methods

### Materials

Curcumin (purity  $\geq 95\%$ ), polyoxyethylene(40)stearate (Myrj 52), ovalbumin (grade V), and acetonitrile (high-pressure liquid chromatography [HPLC] grade) were purchased from Sigma-Aldrich Corporation (St Louis, MO). Aluminum hydroxide gel was obtained from Pierce Chemical Company (Rockford, IL). Stearic acid, lecithin chloroform,

and Tween® 80 were obtained from Sinopharm Chemical Reagent Co, Ltd (Shanghai, China). The water was prepared with a Millipore (Bedford, MA) Milli-Q® system, and all other chemicals were analytical grade.

Balb/c mice (4–5-weeks old,  $20 \pm 2$  g) and specific-pathogen-free, male, Sprague–Dawley rats (4 weeks old, 110–130 g) were purchased from SLAC Laboratory Animal Co, Ltd (Shanghai, China). They were kept in an environmentally controlled room (temperature  $25^\circ\text{C} \pm 2^\circ\text{C}$ , 12 hour light/dark cycle) for 1 week prior to experiments. They were housed under standard humane conditions and had access to food and water ad libitum. All animal procedures were performed according to the protocol approved by the Tongji University Institute of Laboratory Animal Resources.

### Preparation of curcumin-SLNs

Curcumin-SLNs were prepared using the solvent injection method.<sup>22</sup> Briefly, curcumin (150 mg), stearic acid (200 mg), and lecithin (100 mg) were dissolved in 10 mL chloroform in a glass flask (as organic phase). Myrj 52 was dissolved in 30 mL distilled water and heated to  $75^\circ\text{C} \pm 2^\circ\text{C}$  in a water bath (as aqueous phase). The organic phase was injected into the hot aqueous phase under mechanical agitation at 1000 rpm, and the resulting solution was kept at  $75^\circ\text{C}$  with the same agitation speed to remove the organic solvent. The condensed solvent (approximately 5 mL) was then transferred into an equivalent amount of cold water ( $0^\circ\text{C}$ – $2^\circ\text{C}$ ) under continuous mechanical stirring (1000 rpm) for 1.5 hours. The resultant suspension was centrifuged at 20,000 rpm (Avanti J25 centrifuge, JA 25.50 rotor; Beckman Coulter, Palo Alto, USA) to remove the supernatant. The pellet was resuspended in ultrapure water, refrigerated at  $-80^\circ\text{C}$  for 2 hours, and lyophilized in a tabletop lyophilizer.

### Quantifying entrapment efficiency of curcumin by HPLC

The entrapment efficiency (EE) of curcumin in SLNs was determined via HPLC. Briefly, 5 mg of curcumin-SLNs was dissolved in 2 mL of ethanol to extract curcumin. The sample was vortexed for 1 minute, followed by centrifugation at 18,500 g (Centrifuge 5810 R; Eppendorf, Hamburg, Germany) for 10 minutes to obtain a clear supernatant. The supernatant was filtered through a  $0.45\text{-}\mu\text{m}$  membrane and determined by HPLC. Chromatographic conditions were as follows: reverse phase C18 column ( $25\text{ cm} \times 4.6\text{ mm}$ ,  $5\text{ }\mu\text{m}$ ) in Agilent 1100 series equipment (Agilent, Palo Alto, CA); mobile phase, acetonitrile/0.1% trifluoroacetic (1/1, volume [v]/v); flow rate, 0.8 mL/min; detection wavelength, 420 nm. The amount of curcumin in the sample was determined from

the peak area using a calibration curve constructed of standard curcumin. The entrapment efficiency (EE%) and drug loading (DL%) were calculated as follows:

$$EE\% = \frac{W_{\text{total}} - W_{\text{free}}}{W_{\text{total}}} \times 100\%$$

$$DL\% = \frac{W_{\text{total}} - W_{\text{free}}}{W_{\text{lipids}}} \times 100\%$$

where  $W_{\text{free}}$  is the analyzed amount of free drug in the supernatant;  $W_{\text{total}}$  is the theoretical amount of curcumin that was added;  $W_{\text{lipids}}$  is the total amount of lipids.

## Transmission electron microscopy and zeta potential measurements

The surface morphology of curcumin-SLNs was examined by transmission electron microscope (TEM) (JEOL, Tokyo, Japan). A drop of diluted suspension of curcumin-SLNs was placed on a carbon-coated copper TEM grid to form a thin liquid film and then negatively stained with 2% (weight/v) sodium phosphotungstate for 8 minutes and allowed to air dry. The size, polydispersity index (PDI), and zeta potential of curcumin-SLNs were measured by photon correlation spectroscopy (PCS) using a Zetasizer 3000 (Malvern Instruments, Malvern, UK) at 25°C.

## X-ray diffraction study

X-ray diffraction measurements were performed in order to character the crystallographic structure of the curcumin-SLNs, curcumin, and SLNs. The patterns were carried out with an X-ray diffractometer (D8 Advance; Bruker, Karlsruhe, Germany) in the range of 5°–50°. The measurements were performed at a voltage of 40 kV and 25 mA.

## In vitro drug release

The release pattern of curcumin from SLNs was studied using the dialysis membrane method.<sup>23</sup> In detail, 5 mg of curcumin-SLNs dispersed in 2 mL phosphate-buffered saline (PBS) solution was transferred in a dialysis bag (cutoff size, 12 kDa). The bag was then dipped into 100 mL of PBS (containing 10%, v/v, Tween-80) at 37°C in a water bath at 50 rpm. At predetermined time intervals, an aliquot of dialysis medium was removed and the same volume of fresh solution was added. The curcumin concentrations in the released samples were analyzed by an HPLC system as explained above. The release experiments were carried out in triplicate.

## In vivo pharmacokinetic and biodistribution studies

Fifty-six Balb/c mice were randomly divided into two groups. Curcumin and curcumin-SLNs were administered by intraperitoneal injection in a dose equivalent to 400 mg/kg body weight to different groups of the animals. The blood samples were collected via cardiac puncture from four mice at each time point, ranging from 15 minutes to 24 hours postdosing. The blood was then centrifuged at 2800 g for 15 minutes. The resulting plasma was deproteinized by mixing it with a twofold volume of acetonitrile. The curcumin levels were analyzed by HPLC as described above.

Following curcumin and curcumin-SLN administration at 0.5 hours, the spleen, kidney, heart, lung, liver, and brain of the euthanized mice were collected, homogenized, and sonicated in PBS. The curcumin were extracted by adding a twofold volume of acetonitrile. After centrifugation for 10 minutes at 185,000 g, the supernatants were subjected to HPLC analysis. Results were normalized to protein level.

## Sensitization and airway challenge

Forty rats were randomly divided into five groups and received the following treatments separately: (1) sham sensitization plus challenge with saline (nebulization [Neb]); (2) sensitization with OVA via an intraperitoneal (ip) injection plus challenge with OVA via Neb; (3) sensitization with OVA (ip) plus challenge with OVA (Neb) and curcumin (ip); (4) sensitization with OVA (ip) plus challenge with OVA (Neb) and curcumin-SLNs (ip) and (5) sensitization with OVA (ip) plus challenge with OVA (Neb) and SLNs (ip). Briefly, on days 0 and 8, all groups of rats except the normal saline group were sensitized by ip injection of 1 mg OVA precipitated with 10 mg of aluminum hydroxide gel in 1 mL saline. On days 14–21, different groups of rats were injected ip with curcumin, curcumin-SLNs, or SLNs with a dose of 10 mg/kg based on the amount of curcumin. After 0.5 hours, rats were challenged with 1% OVA aerosol generated using an ultrasonic nebulizer (Pro Nebulizer; Pari, Munich, Germany) for 20 minutes in order to maintain sensitivity. On day 22, the pulmonary function testing was performed. A schematic diagram of the treatment schedule is shown in Figure 1.

## Measurement of airway responsiveness to methacholine

The technique for the invasive respiratory function measurements used in this study has been described previously.<sup>24</sup> Airway responsiveness was measured in rats 24 hours after the last challenge in an unrestrained conscious state.

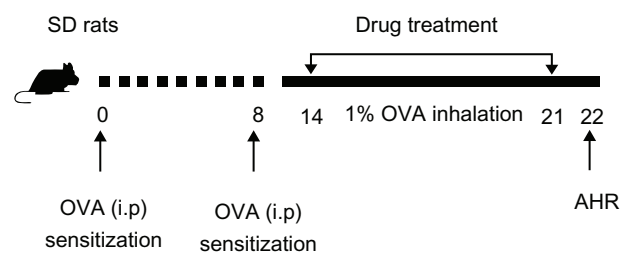


**Figure 1** Experimental protocol for the rat model of allergic asthma.

**Abbreviations:** AHR, airway hyperresponsiveness; i.p, Intraperitoneal injection; OVA, ovalbumin; SD, Sprague–Dawley.

Rats were placed in a supine position and warmed with an incandescent lamp after anesthesia. Methacholine was injected through the jugular vein every 5 minutes at doses of 10, 33, 100, and 330  $\mu\text{g/kg}$ , separately. After each injection, the pulmonary resistance (RL) was calculated over a complete respiratory cycle, using an integration method over flows, volumes, and pressures and were continuously recorded with software (Shanghai Medical College, Fudan University, Shanghai, People's Republic of China) for physiology experiments. The peak response was shown at each concentration of methacholine.

## Lung tissue histopathology

For histological analysis, the rats were sacrificed 24 hours after the final challenge. The lung tissues were fixed in 10% (v/v) neutral buffered formalin for 24 hours at 4°C. The lung tissues were embedded in paraffin, cut into sections of 4  $\mu\text{m}$  thickness, and stained with hematoxylin and eosin (H&E) (Richard-Allan Scientific, Kalamazoo, MI). The slices were evaluated via light microscopy under identical conditions. The degrees of peribronchial and perivascular inflammation were scored in a double-blind screen with two independent blinded investigators using a subjective scale of 0–3 (0, no inflammation was detectable; 1, occasional cuffing with inflammatory cells; 2, most bronchi or vessels surrounded by a thin layer of between one and five inflammatory cells; 3, most bronchi or vessels surrounded by a thick layer of more than five inflammatory cells), as described elsewhere.<sup>25</sup>

## Measurement of T-helper-2 cytokines in bronchoalveolar lavage fluid

Enzyme-linked immunosorbent assays (ELISA) were performed according to the manufacturer's instructions. The level of interleukin (IL)-4 and IL-13 in bronchoalveolar lavage fluid (BALF) were measured with ELISA kits (R&D Systems, Minneapolis, MN).

## Statistics analysis

Results were expressed as mean  $\pm$  standard error of the mean (SEM). Statistical analyses were performed using Student's *t*-test. Values of  $P < 0.05$  or 0.01 were considered statistically significant.

## Results

### Physicochemical characteristics of curcumin-SLNs

As shown in Figure 2A, the curcumin-SLNs were spherical with smooth surfaces. The mean particle size of curcumin-SLNs was found to be  $190.4 \pm 10.6$  nm with a PDI of  $0.276 \pm 0.008$  (Figure 2B). The size of particles measured by PCS was larger than those estimated using TEM. This is because PCS is used for hydrodynamic diameter determination, while TEM is used for characterization of particles in the dried state. Figure 2C shows that the zeta potential of the nanoparticles was  $-20.7 \pm 1.2$  mV. The entrapment efficiency and drug-loading capacity were calculated as  $75\% \pm 4.5\%$  and  $28\% \pm 2.5\%$ , respectively.

### Physical state of curcumin in SLNs

To understand the nature of curcumin after encapsulation into SLNs, the X-ray diffraction method was used. The diffraction patterns of the curcumin, SLNs, and curcumin-SLNs are shown in Figure 3. The pure curcumin exhibited sharp peaks in the range of  $10^\circ$ – $30^\circ$ , which implied a high crystalline structure (Figure 3A), but this characteristic was not observed in the curcumin-SLNs (Figure 3C), which indicates that curcumin entrapped in the lipid core of SLNs was in the amorphous or disordered-crystalline phase.<sup>20</sup> In addition, there was not much difference in the diffraction pattern between SLNs (Figure 3B) and curcumin-SLNs, which suggests that the addition of curcumin had not change the nature of the SLNs.

### In vitro release of curcumin-SLNs

The in vitro drug release profile was carried out in 0.01 M PBS (pH, 7.4) at 37°C. Since curcumin is a highly hydrophobic drug, 10% (v/v) Tween 80 was used in the receptor medium. The result of the release profile of curcumin from nanoparticles is shown in Figure 4. Curcumin-SLNs exhibited a low burst effect with about 22.85% drug released in the first 4 hours, which was due to the release of drugs adsorbed on the surface of nanoparticles. Subsequently, curcumin release profiles displayed a sustained release phase, and about 73% of drug was released at 72 hours. The sustained release could be attributed to the diffusion of drug molecules through the lipid matrix of SLNs.<sup>26</sup>



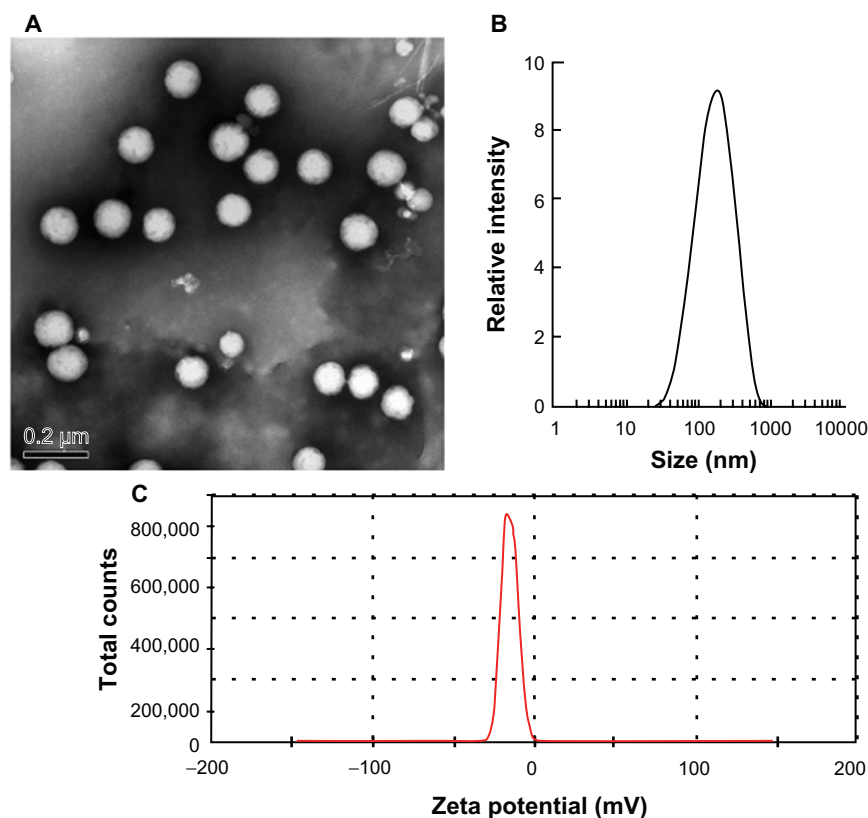


**Figure 2** (A) Transmission electron microscopy photograph of curcumin-SLNs. (B) The particle size distribution of the curcumin-SLNs. (C) Zeta potential distribution of curcumin-SLNs.

**Abbreviation:** SLNs, solid lipid nanoparticles.

## Studies on pharmacokinetics and tissue distribution in mice

The mean plasma concentration–time profiles for the two formulations are illustrated in Figure 5. At all time points, the plasma concentrations in mice treated with curcumin-SLNs were higher than those treated with curcumin. The maximum

concentration value of drug in the curcumin-SLNs (20.85  $\mu\text{M}$ ) was significantly higher than that obtained with curcumin (0.25  $\mu\text{M}$ ). Meanwhile, the area under the curve ( $\text{AUC}_{0-24\text{ h}}$ ) increased by about 26-fold for curcumin-SLNs compared to curcumin. In addition, a second peak of the curcumin concentration was found 2 hours after the administration of the curcumin-SLNs.

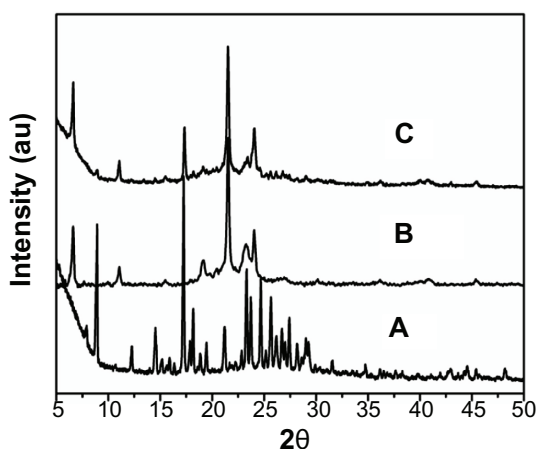


**Figure 3** XRD pattern of (A) native curcumin, (B) blank solid lipid nanoparticles, and (C) curcumin-loaded solid lipid nanoparticles.

**Abbreviation:** XRD, X-ray diffraction.

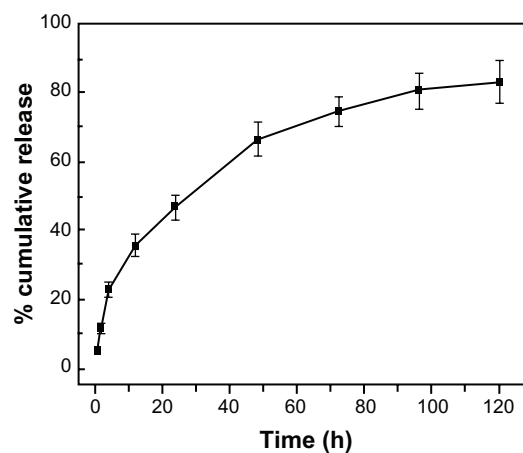


**Figure 4** In vitro release of curcumin from curcumin-loaded solid lipid nanoparticles in PBS (0.01 M, pH 7.4, 10% Tween 80) at 37°C (mean  $\pm$  SEM,  $n = 3$ ).

**Abbreviations:** PBS, phosphate-buffered saline; SEM, standard error of the mean.

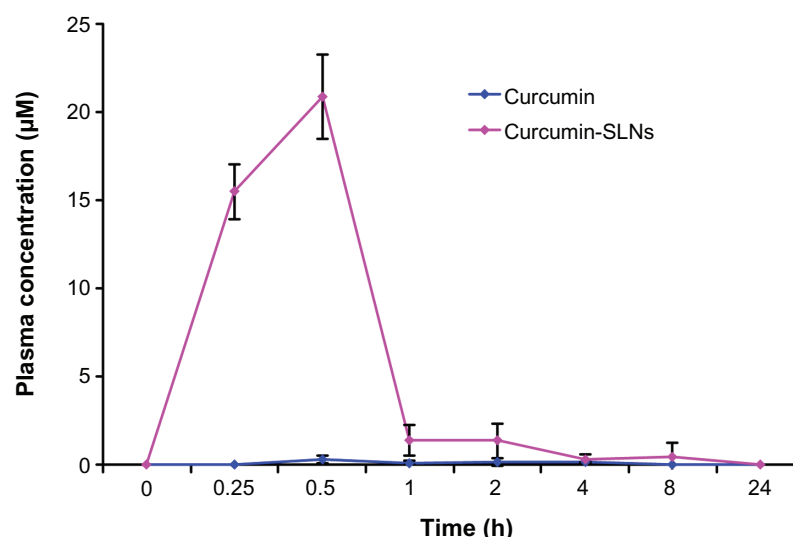


**Figure 5** Plasma curcumin concentration–time curves after intraperitoneal administration of curcumin and curcumin-SLNs to Balb/c mice (400 mg/kg) (mean  $\pm$  SEM,  $n = 4$ ).  
**Abbreviations:** SLNs, solid lipid nanoparticles; SEM, standard error of the mean.

Biodistribution studies were performed to investigate the efficacy of SLNs for delivery of curcumin. As shown in Figure 6, drug in the curcumin-treated group was mainly distributed to the liver and spleen 0.5 hours after injection. However, when administrated with curcumin-SLNs, a significant amount of curcumin was found in all the examined organs, indicating that SLNs could markedly promote enrichment and reduce the distribution of curcumin. Furthermore, the highest drug level was found in liver (10.39 nmol/mg protein) and lung

(7.35 nmol/mg protein), suggesting that SLNs in the blood circulation could be recognized and swallowed as extraneous materials by the mononuclear phagocyte system (MPS), which is prevalent in liver and lung.<sup>22</sup>

### Effect of curcumin-SLNs on AHR

AHR is one of the hallmarks of asthma, although it was regulated by a different set of genes from those controlling immunity and airway inflammation.<sup>27</sup> To determine whether

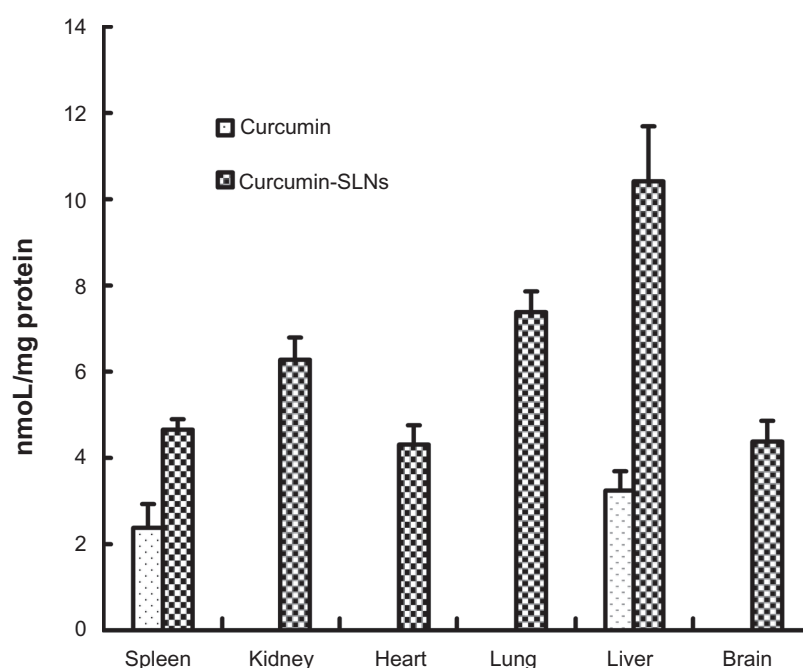


**Figure 6** The distribution of curcumin in organs at 0.5 hours after intraperitoneal administration of curcumin and curcumin-SLNs to Balb/c mice (400 mg/kg) (mean  $\pm$  SEM,  $n = 4$ ).  
**Abbreviations:** SLNs, solid lipid nanoparticles; SEM, standard error of the mean.

curcumin-SLNs could attenuate airway responsiveness efficiently, the clinical parameters of the lung function in response to the increasing concentration of methacholine were measured. As shown in Figure 7, all groups of rats showed increasing bronchial hyperresponsiveness in response to the increasing methacholine concentration. The airway response to methacholine in the OVA-treated group was much higher than the normal saline-treated group ( $P < 0.01$  at 100 and 330  $\mu\text{g/kg}$  methacholine). At 330  $\mu\text{g/kg}$  methacholine, the group treated with curcumin-SLNs significantly suppressed AHR by approximately 66% compared to the asthma group ( $P < 0.01$ ) and by 50% compared to the group treated with native curcumin ( $P < 0.05$ ). The blank solid lipid nanoparticle did not have any effect on the AHR. These results clearly indicated that administration of curcumin-SLNs was more effective than curcumin to attenuate bronchial hyperresponsiveness.

### Effect of curcumin-SLNs on lung tissue

The most direct indicator of airway inflammation was lung histopathology.<sup>28</sup> Therefore, H&E staining was performed to analyze the lung histopathology. As shown in Figure 8A, the lungs of saline-treated rats were normal without inflammatory cells in the airways, whereas the OVA group showed a marked infiltration of inflammatory cells, including eosinophils and

mononuclear cells, in peribronchial and perivascular spaces (Figure 8B). Similarly, the scores for total lung inflammation were significantly increased after OVA inhalation compared with the scores after saline inhalation (Figure 8E). Rats treated with curcumin-SLNs (Figure 8D) showed a significant reduction in peribronchial infiltration of inflammatory cells compared to the other experimental groups (Figure 8B and Figure 8C). In addition, OVA-challenged rats showed more obvious airway wall thickness compared with the saline group, and treatment of curcumin-SLNs could obviously alleviate this airway wall thickness.

### Effect of curcumin-SLNs on the level of IL-4 and IL-13 in BALF

In animal models of asthma, the T-helper-1 (Th1) and T-helper-2 (Th2) cell balance was disturbed and Th2 cells were dominant in the airway.<sup>29</sup> These cells induced immunoglobulin E production and airway inflammation by producing Th2 cytokines, such as IL-4, IL-5, and IL-13.<sup>30</sup> In this work, we examined whether curcumin-SLNs suppressed the expression and secretion of Th2 cytokines more efficiently than curcumin. As shown in Figure 9, the OVA-treated group led to a significant increase in the level of IL-4 ( $84.43 \pm 12.41$  pg/mL) and IL-13 ( $155.39 \pm 15.36$  pg/mL) compared with the saline group (IL-4,  $23.18 \pm 7.61$  pg/mL;

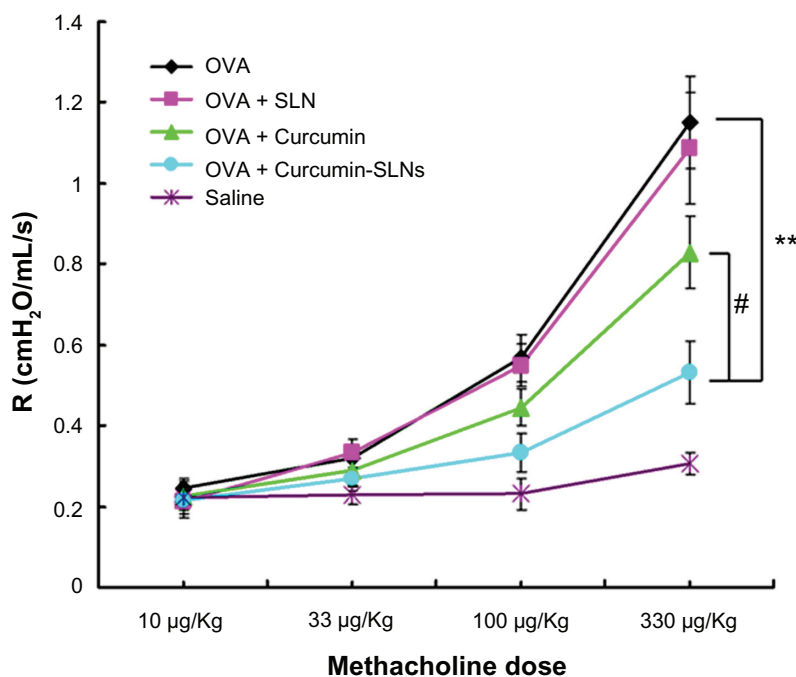


**Figure 7** Effect of curcumin, curcumin-SLNs, and SLNs on airway hyperresponsiveness to inhaled methacholine in OVA-sensitized and OVA-challenged rats.

**Notes:** Airway hyperresponsiveness was obtained from rats 24 hours after the last challenge in response to methacholine at increasing doses (10–330  $\mu\text{g/kg}$ ). The data are expressed as mean  $\pm$  SEM ( $n = 8$ ). #Indicates  $P < 0.05$  compared to the OVA + curcumin group; \*\*Indicates  $P < 0.01$  compared with the OVA group.

**Abbreviations:** OVA, ovalbumin; SLNs, solid lipid nanoparticles.

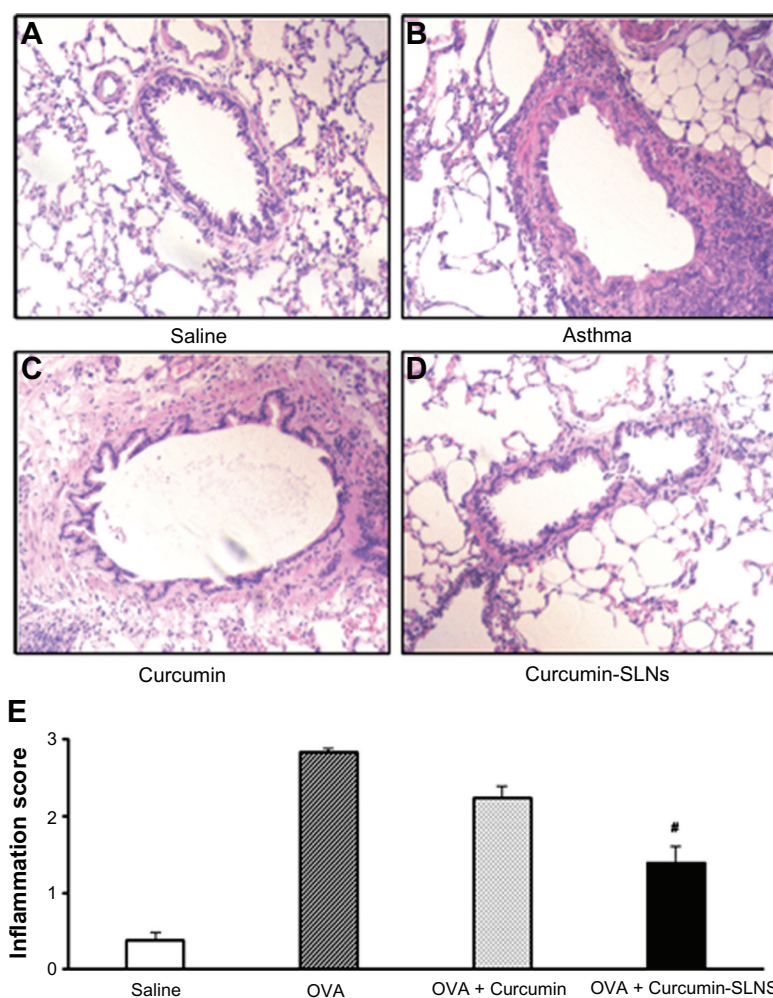


**Figure 8 (A–D)** Representative histological images of hematoxylin and eosin-stained tissue sections from rats treated with normal saline (saline); OVA-sensitized and OVA-challenged rats (OVA); OVA-sensitized and OVA-challenged rats + curcumin treatment (OVA + curcumin); OVA-challenged rats+curcumin-SLNs treatment (OVA + curcumin-SLNs). **(E)** Total lung inflammation scores.

**Note:** #Indicates  $P < 0.05$  compared to the OVA + curcumin group.

**Abbreviations:** OVA, ovalbumin; SLNs, solid lipid nanoparticles.

IL-13,  $43.58 \pm 34.72$  pg/mL). In the curcumin-treated group, cytokine elevation was suppressed and there was a decrease in IL-4 ( $68.19 \pm 12.27$  pg/mL) and in IL-13 ( $108.03 \pm 23.59$  pg/mL). However, the cytokine elevations were more significantly suppressed by curcumin-SLNs (IL-4,  $49.53 \pm 9.05$  pg/mL; IL-13,  $74.97 \pm 27.45$  pg/mL). These findings further demonstrated that curcumin-SLNs have a better anti-inflammatory effect than curcumin.

## Discussion

Asthma is a chronic inflammatory disorder characterized by reversible airway obstruction, bronchial hyperresponsiveness, and airway inflammation.<sup>31</sup> Previous studies have demonstrated the efficacy of curcumin in animal models of asthma,<sup>12,14,32</sup> but its poor solubility limited its clinical efficacy. In recent years, many attempts have been made to improve

the bioavailability of curcumin. As a promising drug-delivery system, SLNs displayed many important advantages, such as controlling drug release and drug targeting, increasing physical stability, high drug loading, and low toxicity.<sup>33,34</sup> Here, we hypothesized that SLN formulation of curcumin was capable of overcoming the above-mentioned drawbacks of curcumin. In the current study, curcumin-SLNs were developed to serve as an alternative formulation of curcumin for a more effective therapy of asthma.

Since the physicochemical properties of nanoparticles influenced their physical stability, cellular uptake, and biodistribution in vivo, it was very important to evaluate their physicochemical parameters.<sup>35</sup> First, we observed their size distribution and surface charge. The average particle size was about 190 nm in diameter with a narrow distribution. The surface charge of the nanoparticles was of



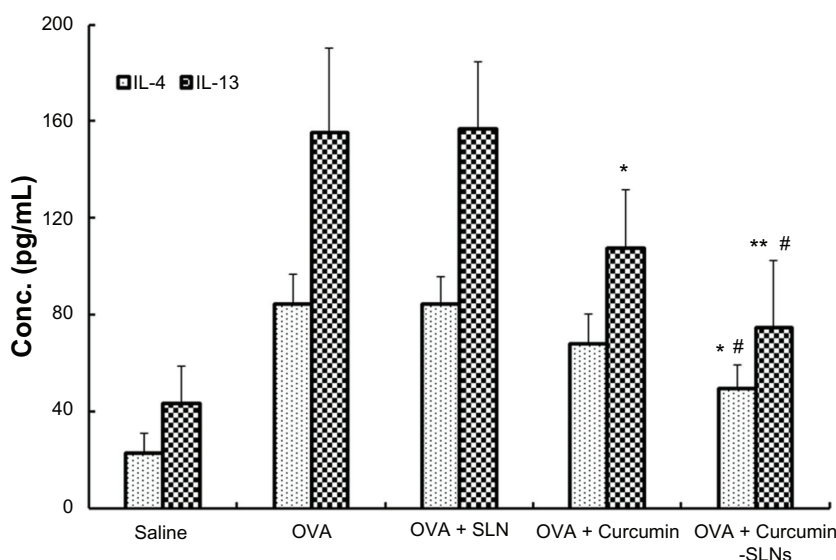


**Figure 9** Effect of curcumin, curcumin-SLNs, and SLNs on IL-4 and IL-13 expression in BALF collected from OVA-sensitized and OVA-challenged rats.

**Notes:** BALF was collected 24 hours after the last challenge in the normal saline group (saline), OVA-sensitized and OVA-challenged rats (OVA); OVA-sensitized and OVA-challenged rats + curcumin treatment group (OVA + curcumin); OVA-challenged rats + curcumin-SLNs treatment group (OVA + curcumin-SLNs). The data are expressed as mean  $\pm$  SEM ( $n = 8$ ). \*Indicates  $P < 0.05$  compared to the OVA group; \*\*Indicates  $P < 0.01$  compared to the OVA group; #indicates  $P < 0.05$  compared to the OVA + curcumin group.

**Abbreviations:** SLN, solid lipid nanoparticles; IL, interleukin; BALF, bronchoalveolar lavage fluid; OVA, ovalbumin; SEM, standard error of the mean.

interest since it influenced the stability of the nanoparticle suspension.<sup>36</sup> In this study the zeta potential of a nanoparticle was  $-20.7 \pm 1.2$  mV, which was high enough to make the nanoparticles repel each other, thereby avoiding particle aggregation and keeping the long-term stability of nanoparticles.<sup>37,38</sup> Second, X-ray diffraction was used to investigate the nature of curcumin after encapsulation into the SLNs. It was observed that curcumin entrapped in the lipid core of the SLN was in the amorphous or disordered-crystalline phase. The phase facilitates sustained release of the drug from the nanoparticles.<sup>35</sup>

In *in vivo* pharmacokinetics studies, the curcumin-SLN-treated group showed a higher plasma concentration of curcumin than the curcumin-treated group. It has been reported that the drug when encapsulated into the nanoformulation, which exhibits sustained release, could change the drug pharmacokinetics and improve drug efficacy.<sup>39,40</sup> Indeed, the release pattern of our formulation typically showed an initial burst release followed by a prolonged release over several hours. This could prolong the drug retention time in blood,<sup>41</sup> thereby increasing the drug concentration in targeted organs. A similar phenomenon was observed after the intravenous administration of oridonin-SLNs in rabbits.<sup>42</sup> In addition, a second peak at 2 hours in the pharmacokinetic profile of the curcumin-SLNs was also observed, possibly related to a prolonged absorption of curcumin from the bioadhesion of the nanoparticles to the gut. The similar two-peak drug

concentration time curves had also been reported in the pharmacokinetic study of oral administration of puerarin-SLNs.<sup>22</sup>

The results of tissue distributions in our studies showed that SLNs could apparently increase the tissue distributions of curcumin, especially in the liver and lung. Previous studies had also revealed that SLNs might be a promising lung-targeting drug carrier for lipophilic drugs, such as dexamethasone acetate.<sup>43</sup> SLNs composed of phospholipid are suitable for targeting drug into the lung. By lowering the tensile force of the alveolus surface, phospholipids could speed the spread of drug droplets and the disaggregation of solid lipid so that drugs on the alveolus surface could be absorbed rapidly.<sup>44</sup>

To further determine whether the curcumin-SLNs showed efficient therapeutic effects on lung disease, an *in vivo* animal asthma model was conducted. The airway responsiveness was one of the most important clinical discoveries in asthma studies.<sup>29</sup> The methacholine challenge was a useful tool in diagnosis of allergic respiratory disorders, which had been widely used in assessing airway responsiveness.<sup>45</sup> In the present study, OVA sensitization and challenge evoked a significant hyperresponsiveness to methacholine challenge in sensitized rats. Curcumin was found to inhibit the airway hyperreactivity. The results were in agreement with the report that curcumin was effective in improving the impaired airway features in the

OVA-sensitized guinea pigs.<sup>13</sup> Surprisingly, rats treated with curcumin-SLNs exhibited much lower airway hyperreactivity, which might be attributed to the following reasons: (1) Encapsulation of curcumin into SLN enhanced the bioavailability of curcumin and exerted a profound influence on the pharmacokinetics of the drug; (2) Encapsulation of curcumin into SLNs resulted in higher accumulation of curcumin in lung so that more drugs reached the inflamed tissue to exert their therapeutic effect.

As we know, the presence of increased numbers of eosinophils is a hallmark of asthma.<sup>46</sup> Compared with curcumin-treated rats, curcumin-SLN-treated rats had significantly reduced eosinophilia in lung tissue. This effect might result from a decrease in the levels of Th2 cytokines responsible for eosinophil recruitment into the lung in asthma. We therefore measured Th2 cytokines, such as IL-4 and IL-13, in BALF. IL-4 is important in maintaining the Th2 phenotype. IL-13, although not directly supportive of Th2 differentiation, is also involved in the modulation of eosinophilic inflammation and airway smooth muscle hyperplasia, the induction of goblet-cell hyperplasia, the recruitment of monocytes and T cells, and the induction of a corticosteroid-insensitive airway inflammation.<sup>47</sup> The results of our study showed that OVA sensitization and challenge led to a significant increase in the level of IL-4 and IL-13 in rats. This kind of increase could be alleviated by curcumin. Previous studies have also reported that curcumin might have a potential effect on controlling allergic diseases through inhibiting the production of Th2 cytokines.<sup>32</sup> Curcumin entrapped in SLNs could more effectively suppress the generation of key Th2-type cytokines than curcumin alone. These results provide further evidence that curcumin-SLNs could better enhance the therapeutic effects on asthma compared to curcumin by increasing the distribution of curcumin in the lung.

## Conclusion

In the present study, curcumin-SLNs were successfully prepared by the solvent injection method. The formulation with ideal encapsulation efficiency had a mean particle size of about 190 nm. An in vitro release study indicated that curcumin-SLNs exhibited sustained release after an initial burst release. The biodistribution studies demonstrated that SLNs could significantly increase the lung uptake efficiency of curcumin. In addition, compared to the curcumin-treated group, administration of curcumin-SLNs into OVA-induced asthmatic rats showed a significant reduction in the AHR and the number of inflammatory cells in lung tissue. We conclude from these results that SLNs could serve as a promising

delivery system to enhance the therapeutic effect of curcumin in the treatment of asthma.

## Acknowledgments

The work was financially supported by the 973 project of the Ministry of Science and Technology (Grant No 2010CB912604, 2010CB933901), National Natural Science Foundation of China (Grant No 31140038), Science and Technology Commission of Shanghai Municipality (Grant No 11411951500), and Research Fund for the Doctoral Program of Higher Education of China (Grant No 20090072120019) and the Fundamental Research Funds for the Central Universities of China.

## Disclosure

The authors report no conflicts of interest in this work.

## References

1. Yin LM, Jiang GH, Wang Y, et al. Use of serial analysis of gene expression to reveal the specific regulation of gene expression profile in asthmatic rats treated by acupuncture. *J Biomed Sci.* 2009;16(46): 1–13.
2. Ray A, Cohn L. Th2 cells and GATA-3 in asthma: new insights into the regulation of airway inflammation. *J Clin Invest.* 1999;104(8): 985–993.
3. Yin LM, Jiang GH, Wang Y, et al. Serial analysis of gene expression in a rat lung model of asthma. *Respirology.* 2008;13(7):972–982.
4. Edwards MR, Bartlett NW, Clarke D, Birrell M, Belvisi M, Johnston SL. Targeting the NF-kappaB pathway in asthma and chronic obstructive pulmonary disease. *Pharmacol Ther.* 2009;121(1):1–13.
5. Inapagolla R, Guru BR, Kurtoglu YE, Gao X, Lieh-Lai M, et al. In vivo efficacy of dendrimer-methylprednisolone conjugate formulation for the treatment of lung inflammation. *Int J Pharm.* 2010;399(1–2): 140–147.
6. Strehle EM. Long-term management of children with neuromuscular disorders. *J Pediatr (Rio J).* 2009;85(5):379–384.
7. Matsuo Y, Ishihara T, Ishizaki J, Miyamoto K, Higaki M, Yamashita N. Effect of betamethasone phosphate loaded polymeric nanoparticles on a murine asthma model. *Cell Immunol.* 2009;260(1):33–38.
8. Butoescu N, Seemayer CA, Foti M, Jordan O, Doelker E. Dexamethasone-containing PLGA superparamagnetic microparticles as carriers for the local treatment of arthritis. *Biomaterials.* 2009;30(9): 1772–1780.
9. Lee JH, Kim JW, Ko NY, et al. Curcumin, a constituent of curry, suppresses IgE-mediated allergic response and mast cell activation at the level of Syk. *J Allergy Clin Immunol.* 2008;121(5): 1225–1231.
10. Tsai YM, Chien CF, Lin LC, Tsai TH. Curcumin and its nano-formulation: the kinetics of tissue distribution and blood-brain barrier penetration. *Int J Pharm.* 2011;416(1):331–338.
11. Suzuki M, Nakamura T, Iyoki S, et al. Elucidation of anti-allergic activities of curcumin-related compounds with a special reference to their anti-oxidative activities. *Biol Pharm Bull.* 2005;28(8):1438–1443.
12. Moon DO, Kim MO, Lee HJ, et al. Curcumin attenuates ovalbumin-induced airway inflammation by regulating nitric oxide. *Biochem Biophys Res Commun.* 2008;375(2):275–279.
13. Ram A, Das M, Ghosh B. Curcumin attenuates allergen-induced airway hyper-responsiveness in sensitized guinea pigs. *Biol Pharm Bull.* 2003;26(7):1021–1024.

14. Oh SW, Cha JY, Jung JE, et al. Curcumin attenuates allergic airway inflammation and hyper-responsiveness in mice through NF-kappaB inhibition. *J Ethnopharmacol*. 2011;136(3):414–421.
15. Anand P, Kunnumakkara AB, Newman RA, Aggarwal BB. Bioavailability of curcumin: problems and promises. *Mol Pharm*. 2007;4(6):807–818.
16. Pan MH, Huang TM, Lin JK. Biotransformation of curcumin through reduction and glucuronidation in mice. *Drug Metab Dispos*. 1999;27(4):486–494.
17. Sharma RA, Steward WP, Gescher AJ. Pharmacokinetics and pharmacodynamics of curcumin. *Adv Exp Med Biol*. 2007;595:453–470.
18. Farboud ES, Nasrollahi SA, Tabbakhi Z. Novel formulation and evaluation of a Q10-loaded solid lipid nanoparticle cream: in vitro and in vivo studies. *Int J Nanomedicine*. 2011;6:611–617.
19. Xie S, Pan B, Shi B, et al. Solid lipid nanoparticle suspension enhanced the therapeutic efficacy of praziquantel against tapeworm. *Int J Nanomedicine*. 2011;6:2367–2374.
20. Mulik RS, Monkkonen J, Juvonen RO, Mahadik KR, Paradkar AR. Transferrin mediated solid lipid nanoparticles containing curcumin: Enhanced in vitro anticancer activity by induction of apoptosis. *Int J Pharm*. 2010;398(1–2):190–203.
21. Kakkar V, Kaur IP. Evaluating potential of curcumin loaded solid lipid nanoparticles in aluminium induced behavioural, biochemical and histopathological alterations in mice brain. *Food Chem Toxicol*. 2011;49(11):2906–2913.
22. Luo CF, Yuan M, Chen MS, et al. Pharmacokinetics, tissue distribution and relative bioavailability of puerarin solid lipid nanoparticles following oral administration. *Int J Pharm*. 2011;410(1–2):138–144.
23. Avgoustakis K, Beletsi A, Panagi Z, Klepetsanis P, Karydas AG, Ithakissios DS. PLGA-mPEG nanoparticles of cisplatin: in vitro nanoparticle degradation, in vitro drug release and in vivo drug residence in blood properties. *J Control Release*. 2002;79(1–3):123–135.
24. Yin LM, Li HY, Zhang QH, et al. Effects of S100A9 in a rat model of asthma and in isolated tracheal spirals. *Biochem Biophys Res Commun*. 2010;398(3):547–552.
25. Gueders MM, Balbin M, Rocks N, et al. Matrix metalloproteinase-8 deficiency promotes granulocytic allergen-induced airway inflammation. *J Immunol*. 2005;175(4):2589–2597.
26. Jain A, Agarwal A, Majumder S, et al. Mannosylated solid lipid nanoparticles as vectors for site-specific delivery of an anti-cancer drug. *J Control Release*. 2010;148(3):359–367.
27. Wang X, Xu W, Kong X, et al. Modulation of lung inflammation by vessel dilator in a mouse model of allergic asthma. *Respir Res*. 2009;10(66):1–8.
28. Wang X, Xu W, Mohapatra S, et al. Prevention of airway inflammation with topical cream containing imiquimod and small interfering RNA for natriuretic peptide receptor. *Genet Vaccines Ther*. 2008;6(7):1–9.
29. Han B, Guo J, Abrahaley T, et al. Adverse effect of nano-silicon dioxide on lung function of rats with or without ovalbumin immunization. *PLoS One*. 2011;6(2):e17236.
30. Park HJ, Lee CM, Jung ID, et al. Quercetin regulates Th1/Th2 balance in a murine model of asthma. *Int Immunopharmacol*. 2009;9(3):261–267.
31. Lee MY, Seo CS, Ha H, et al. Protective effects of *Ulmus davidiana* var. *japonica* against OVA-induced murine asthma model via upregulation of heme oxygenase-1. *J Ethnopharmacol*. 2010;130(1):61–69.
32. Kurup VP, Barrios CS, Raju R, Johnson BD, Levy MB, Fink JN. Immune response modulation by curcumin in a latex allergy model. *Clin Mol Allergy*. 2007;5(1):1–12.
33. Kuo YC, Liang CT. Inhibition of human brain malignant glioblastoma cells using carmustine-loaded cationic solid lipid nanoparticles with surface anti-epithelial growth factor receptor. *Biomaterials*. 2011;32(12):3340–3350.
34. Lee MK, Lim SJ, Kim CK. Preparation, characterization and in vitro cytotoxicity of paclitaxel-loaded sterically stabilized solid lipid nanoparticles. *Biomaterials*. 2007;28(12):2137–2146.
35. Mohanty C, Sahoo SK. The in vitro stability and in vivo pharmacokinetics of curcumin prepared as an aqueous nanoparticulate formulation. *Biomaterials*. 2010;31(25):6597–6611.
36. Hu FX, Neoh KG, Kang ET. Synthesis and in vitro anti-cancer evaluation of tamoxifen-loaded magnetite/PLLA composite nanoparticles. *Biomaterials*. 2006;27(33):5725–5733.
37. Misra R, Acharya S, Dilnawaz F, Sahoo SK. Sustained antibacterial activity of doxycycline-loaded poly(D,L-lactide-co-glycolide) and poly(epsilon-caprolactone) nanoparticles. *Nanomedicine (Lond)*. 2009;4(5):519–530.
38. Sahoo SK, Panyam J, Prabha S, Labhasetwar V. Residual polyvinyl alcohol associated with poly (D,L-lactide-co-glycolide) nanoparticles affects their physical properties and cellular uptake. *J Control Release*. 2002;82(1):105–114.
39. Zhang C, Qu G, Sun Y, Wu X, et al. Pharmacokinetics, biodistribution, efficacy and safety of N-octyl-O-sulfate chitosan micelles loaded with paclitaxel. *Biomaterials*. 2008;29(9):1233–1241.
40. Manjunath K, Venkateswarlu V. Pharmacokinetics, tissue distribution and bioavailability of clozapine solid lipid nanoparticles after intravenous and intraduodenal administration. *J Control Release*. 2005;107(2):215–228.
41. Gao Y, Xu P, Chen L, Li Y. Prostaglandin E1 encapsulated into lipid nanoparticles improves its anti-inflammatory effect with low side-effect. *Int J Pharm*. 2010;387(1–2):263–271.
42. Zhang DR, Tan TW, Gao L. Preparation of oridonin-loaded solid lipid nanoparticles and studies on them in vitro and in vivo. *Nanotechnology*. 2006;17:5821–5828.
43. Xiang QY, Wang MT, Chen F, et al. Lung-targeting delivery of dexamethasone acetate loaded solid lipid nanoparticles. *Arch Pharm Res*. 2007;30(4):519–525.
44. Du B, Li Y, Li X, A Y, Chen C, Zhang Z. Preparation, characterization and in vivo evaluation of 2-methoxyestradiol-loaded liposomes. *Int J Pharm*. 2010;384(1–2):140–147.
45. Brusasco V, Crimi E. Methacholine provocation test for diagnosis of allergic respiratory diseases. *Allergy*. 2001;56(12):1114–1120.
46. Lee M, Kim S, Kwon OK, Oh SR, Lee HK, Ahn K. Anti-inflammatory and anti-asthmatic effects of resveratrol, a polyphenolic stilbene, in a mouse model of allergic asthma. *Int Immunopharmacol*. 2009;9(4):418–424.
47. Therien AG, Bernier V, Weicker S, et al. Adenovirus IL-13-induced airway disease in mice: a corticosteroid-resistant model of severe asthma. *Am J Respir Cell Mol Biol*. 2008;39(1):26–35.

## International Journal of Nanomedicine

### Publish your work in this journal

The International Journal of Nanomedicine is an international, peer-reviewed journal focusing on the application of nanotechnology in diagnostics, therapeutics, and drug delivery systems throughout the biomedical field. This journal is indexed on PubMed Central, MedLine, CAS, SciSearch®, Current Contents®/Clinical Medicine,

Submit your manuscript here: <http://www.dovepress.com/international-journal-of-nanomedicine-journal>

Dovepress

Journal Citation Reports/Science Edition, EMBase, Scopus and the Elsevier Bibliographic databases. The manuscript management system is completely online and includes a very quick and fair peer-review system, which is all easy to use. Visit <http://www.dovepress.com/testimonials.php> to read real quotes from published authors.